Reconfigurable UWB Antenna With RF-MEMS for On-Demand WLAN Rejection

Dimitris E. Anagnostou, *Senior Member, IEEE*, Michael T. Chryssomallis, *Senior Member, IEEE*, Benjamin D. Braaten, *Member, IEEE*, John L. Ebel, *Member, IEEE*, and Nelson Sepúlveda, *Senior Member, IEEE*

***Abstract*—A MEMS reconfigurable ultra-wideband (UWB) antenna that rejects on-demand all WLAN signals in the entire 5.15 to 5.825 GHz range (675 MHz bandwidth) is presented. The antenna design, miniaturization procedure, and monolithic integration with the MEMS and biasing network on SiO_2 Quartz substrate are described. The integration challenges are addressed and the work is presented in a way that is useful for antenna engineers. A method to vary the rejection bandwidth is also provided. The fabricated prototype is conformal and single-sided. The antenna is measured using a custom-built platform at a university laboratory. Results indicate a successful integration and minimal interference of the MEMS and biasing circuitry with the antenna, paving the road for more integrated reconfigurable antennas on SiO_2 using MEMS technology. Such antennas can improve UWB, WLAN and cognitive radio communication links.**

***Index Terms*—Antennas, cognitive radio, integrated components, MEMS, reconfigurable antennas.**

I. Introduction

BAND-REJECT ultra-wideband (UWB) antennas can facilitate UWB systems to minimize in-band interferences within their bandwidth, extended from 3.1 to 10.6 GHz [1]. Interferences often originate from the increased use of IEEE 802.11n (and the older 802.11a) WLANs that allocate channels between 5.15 and 5.825 GHz. WLAN devices that transmit in the above range with increased signal intensity interfere with nearby UWB receivers, while in a different scenario, radiation from UWB transmitters may interfere with WLAN devices that receive a weak WLAN signal. To mitigate these interferences, UWB antennas that permanently reject WLAN bands have been developed. However rejection is not always necessary. Better UWB link efficiency requires rejection to occur on-demand when the WLAN signal is present. Using a single reconfigurable antenna is the proposed solution to this problem. In this work we develop the needed MEMS reconfigurable UWB antenna that can reject on-demand the 5.15–5.825 GHz 802.11a/n WLAN bands.

The design is based on a traditional uni-planar disc-shaped UWB monopole. For this development, several challenges are addressed: (a) pin diodes are difficult to bias because the design lacks a backside ground plane behind the monopole. This uni-planar structure however makes it ideal to monolithically-integrate MEMS. (b) MEMS can be biased using $\lambda/4$ microstrip lines and stubs, grounded vias, or high-resistive lines. The first two typically require a backside ground plane, which single-sided monopoles do not have. The third option motivated the development of high-resistive bias lines on SiO_2 (Quartz) substrate and led to the monolithic integration of the MEMS on-wafer with the bias lines and the antenna. (c) This integration also helped avoid using bulkier pre-packaged off-the-shelf MEMS that need wire-bonds that could affect the antenna pattern and impedance.

Such on-demand WLAN rejection antennas have not yet been realized, possibly due to difficulties in their design and integration. Here we describe the design and integration of such an antenna with MEMS, as well as the fabrication of a prototype, and measurements. A comparison with current state of the art is made in Section II and results are compared in Section V.

II. Band-Notched UWB Antennas Literature

During the last years, many prototypes of band-reject UWB antennas have been proposed. Most are not reconfigurable antennas, so they do not include MEMS or other reconfiguration means (pin diodes, varactors, etc). Among them, some characteristic prototypes that involve permanent rejection mechanisms can be found in [2]–[12]. Most design approaches involve permanent rejection using slots [3], [5], stubs [8], [9], and feed line or ground modifications (i.e., using resonators) [11], [12]. Designs of interest include a dual-notched monopole with parasitic $\lambda/4$ resonant stubs and strong rejection especially in the

Manuscript received March 02, 2012; revised November 08, 2013; accepted November 12, 2013. Date of publication November 27, 2013; date of current version January 30, 2014. This work was supported in part by the Defense Advanced Research Projects Agency/ MTO Young Faculty Award under agreement number N66001-11-1-4145, the US Army Research Office under agreement number W911NF-09-1-0277, the National Science Foundation under collaborative grants ECS-1310400 and ECS-1310257, the Air Force Research Laboratories/SAIC under contract No. FA9453-08-C-0245, the Greek Ministry of Education project THALES RF-Eigen-Sdr, and the Air Force Research Laboratories/MacAulay-Brown Inc. under agreement number MacB-07-D-0016 Task Order 0010.

D. E. Anagnostou is with the Electrical and Computer Engineering Department, South Dakota School of Mines and Technology, Rapid City, SD 57701 USA and also with the Democritus University of Thrace, Xanthi 67100, Greece (e-mail: danagn@ieee.org).

M. T. Chryssomallis is with the Electrical and Computer Engineering Department, Democritus University of Thrace, Xanthi 67100, Greece (e-mail: mchrysso@ee.duth.gr).

B. D. Braaten is with the Electrical and Computer Engineering Department, North Dakota State University, Fargo, ND 58102 USA (e-mail: benjamin.braaten@ndsu.edu).

J. L. Ebel is with the Air Force Research Laboratory, Sensors Directorate, Wright-Patterson Air-Force Base, OH 45433 USA (e-mail: John.Ebel@us.af.mil).

N. Sepulveda is with the Electrical and Computer Engineering, Michigan State University, East Lansing, MI 48823 USA (e-mail: nelsons@egr.msu.edu).

Color versions of one or more of the figures in this paper are available online at http://ieeexplore.ieee.org.

Digital Object Identifier 10.1109/TAP.2013.2293145

first band [10]; a triple-band rejection with Ω-shaped slots and additional slits on a defective ground plane [11]; and resonant loops placed adjacent to the feed line to trap different frequencies that achieved similar levels of rejection [12]. Both [11] and [12] achieve strong rejection and with sharp roll-off, but they are not single-sided. Thus, they require double-sided etching that may impose limitations if the antenna is to be made reconfigurable, for example in a potential integration with MEMS, while the curved slits make them difficult to fine-tune. Moreover, most previous works focus on rejecting only a portion of the WLAN spectrum (i.e., either the 5.25 GHz band or the 5.75 GHz band) [2], [3], [5], [7], while prototypes that reject all WLAN usually employ multiple bands rejection [2], [6], [9], [11], [12]. In all these works, a narrowband (e.g., 100 to 200 MHz) rejection with a single resonator can indeed achieve a strong rejection level (about 10 to 20 dB). The rejection of wider bandwidths (e.g., 400 to 700 MHz) is more limited to values close to 3 or 4 dB, as in [2], [13]. The proposed antenna aims at wideband rejections of the 675 MHz WLAN band and with sharp roll-off, as in [2], [13]. Also, a method to vary the bandwidth of the rejected frequencies is mentioned in Section III. To better comprehend the significance of this work, the results, which are presented in Section V, are compared with prior studies aiming similar functionalities (i.e., UWB antennas that reject the WLAN), and the performance of the developed antenna is found comparable to or better than these prior studies of band-reject antennas that did or did not face the challenges of MEMS integration [2], [3], [5], [6], [10], [12], [13].

Successful implementations of UWB antennas with reconfigurable WLAN rejection with diodes or varactors have not yet appeared. Some implementations however use diodes to reconfigure rejection [14]–[16], but involve different design goals: 1) radiate from different frequencies (1.5–5 GHz [14] or 2.5–8 GHz [15]), 2) have larger antenna dimensions (e.g., 75 × 38.85 mm [15]), 3) have larger rejected bandwidth (from 1–2 GHz [14] or up to 4 GHz [15]), 4) achieve high relative rejection (more than 10 dB [14] or up to 30 dB [15]), 5) are designs with directional patterns [14]–[16] potentially unsuitable for receivers, and most important 6) do not require the sharp roll-off imposed by the current WLAN-only rejection that approximates the ideal brick-wall filter, and therefore they cannot be directly compared to this work.

Compared to pin diodes, RF-MEMS may require two bias lines (instead of one) to actuate but provide high linearity and low losses. Their integration however up to now is limited mainly to laboratory prototypes and only one UWB antenna with MEMS reconfigurable rejection has been reported [13], which presented patterns using ideal reference prototypes. Here, measured patterns using the integrated MEMS during 'on' and 'off' actuation were made for the first time in a university setting and are presented.

This work differs also from prior MEMS antennas [17]–[22] mostly in the MEMS design, use, substrate and application which is the on-demand rejection of WLAN interference. The MEMS employ a new membrane design with dimples and can be used to reject any (one here) frequency band instead of enabling or fine-tuning additional ones. In fact, the MEMS here are not limited by a narrowband bias network, and so they can be used to reject any desired frequency. This work also presents the development of high-resistive lines on SiO_2 for the first time, and complements the preliminary results of [23], by providing: a) new, accurate $|S_{11}|$ measurements and how they were taken, b) the antenna measurement platform and patterns measured during MEMS actuation, for the first time in a university laboratory, c) a concise antenna design and matching methodology, d) MEMS 3-D diagrams, e) a method to vary the rejection bandwidth and f) an equivalent circuit model for both MEMS states.

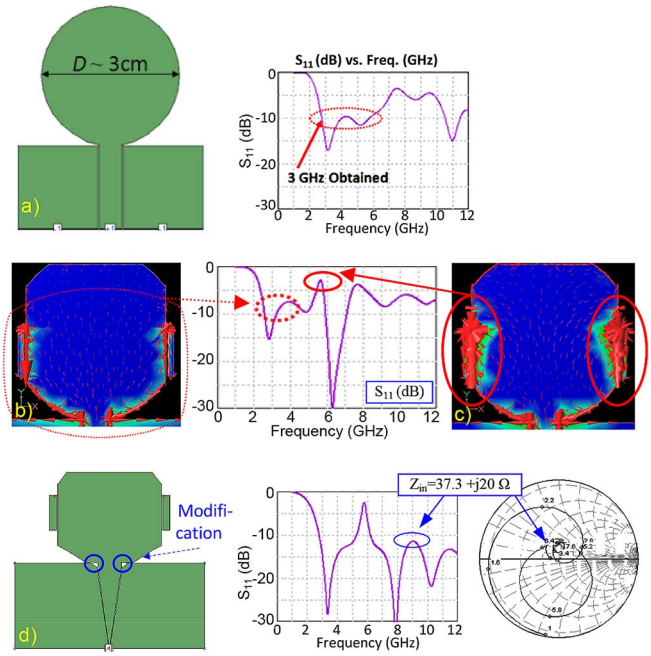

Fig. 1. (a)–(d). (a) The initial design and its $|S_{11}|$, (b)–(c) intermediate steps toward linearization and size reduction, illustrating the surface currents at (b) 3 GHz showing no flow on the top part of the antenna that can therefore be removed, and at (c) 5.6 GHz showing most current concentrated around the $\lambda_g/4$ stubs, so this frequency is being rejected; (d) final stage of the design and matching of the band-reject reconfigurable antenna.

III. Antenna Design and Matching

The base design for this antenna is a CPW-fed disc-shaped monopole with diameter 3 cm designed on SiO_2 substrate with permittivity $\varepsilon_r = 3.9$ (Fig. 1(a)). Its lowest well-matched frequency is 3 GHz. The antenna is fed by a 50 Ω CPW line that is tapered from a 5000 μm to a 100 μm width (CPW gaps from 150 μm down to 12 μm) for compatibility with the available 250-μm pitch GSG RF probe and to minimize losses throughout.

Two quarter-wave open-circuited stubs are added to the edges of the antenna to facilitate the band-notched behavior at the frequencies when they appear as short circuits connected to the antenna structure. The initially curved stubs were replaced by linear ones for easy fabrication and adjustment. Thin stubs (e.g., 200 μm wide) provide narrowband rejection, whereas the wider stubs (e.g., 1500 μm) used here reject the entire 5.15–5.825 GHz bandwidth. This happens because there is more than a single frequency at which the RF current 'sees' a length of one quarter-wave stub. This rule of thumb can be used to adjust or vary the rejection bandwidth. Next, the antenna edges were also linearized for the stubs to maintain a fixed distance from

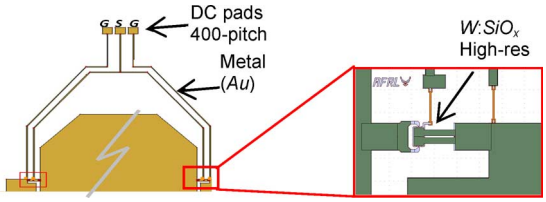

Fig. 2. Schematic (not to scale) of the MEMS bias network. On top are the DC pads that the DC probes bias. The inset shows the RF model of the switch.

them [24]. The feed structure is then modified by narrowing the opening near the antenna and introducing two triangular slots of 250 μm each orthogonal side to reduce reactive loading and lower the input resistance. Lastly, the monopole height is further reduced by about 20% by removing metal from parts with low current density (Fig. 1(b),(c)). Fig. 1(d) shows the final design and its simulated S_{11}.

The MEMS biasing network layout is discussed in Section IV but for completeness it is shown in Fig. 2. It is worth to note that the use of diodes instead of MEMS would introduce a series resistance that improves rejection and broadens bandwidth, but also reduces roll-off, steepness and Q, as observed also in [14].

IV. RF-MEMS Fabrication and Antenna Integration

The MEMS fabrication and associated 3-D layouts are shown in Fig. 3(a)–(d) with mask layouts on the right column. The process follows the general path described in [23] but contains membrane and bias line novelties. Fabrication begins with a *Ti*/*Au* 20/280 nm e-beam evaporation and standard photolithography patterning to define the antenna, stubs, bias lines and MEMS electrode. The cantilever will be anchored at the stub end (RF OUT).

For the biasing lines, simulations pertinent to their sheet resistance showed that 10 KΩ/sq suffice to suppress the 5.5 GHz RF current propagation to less than 100 μm ($\sim \lambda/20$) before attenuating by 30 dB. This led to the development of high-resistive lines on SiO_2, for the first time. The lines are defined with Tungsten deposited into W:SiO_x silica matrix at a ratio 1:4.6 (Fig. 3(a)), and provide about 10 KΩ/sq at room temperature. The resistive part is 10 nm thick, 8 μm wide and 160 μm long and was deposited by a Discovery-22 Sputterer at 20°C, which is notably lower than the 850°C needed for the more expensive CCVD process of AZO lines [19]. This also helps avoid floating grounds that were used in replacement of these lines with LCP substrate due to its 290°C temperature limitation [22]. All remaining parts are electroplated *Au*.

The second novelty is the membrane design that employs dimples that are the only parts of the cantilever that contact the antenna when the switch is actuated. The dimples (0.6 μm deep holes) are patterned on the 1.2 μm thick PMGI sacrificial layer (Fig. 3(b)) that is spun and patterned to define the anchor location and create the 1.2 μm cantilever-electrode gap. After a 6 μm thick electroplating and patterning, this creates two 0.6 μm posts (dimples) under the cantilever and two 0.6 μm shallow valleys at its surface. As the membrane is 6 μm thick, the 10% thickness non-uniformity is small and does not affect the structural integrity of the switch.

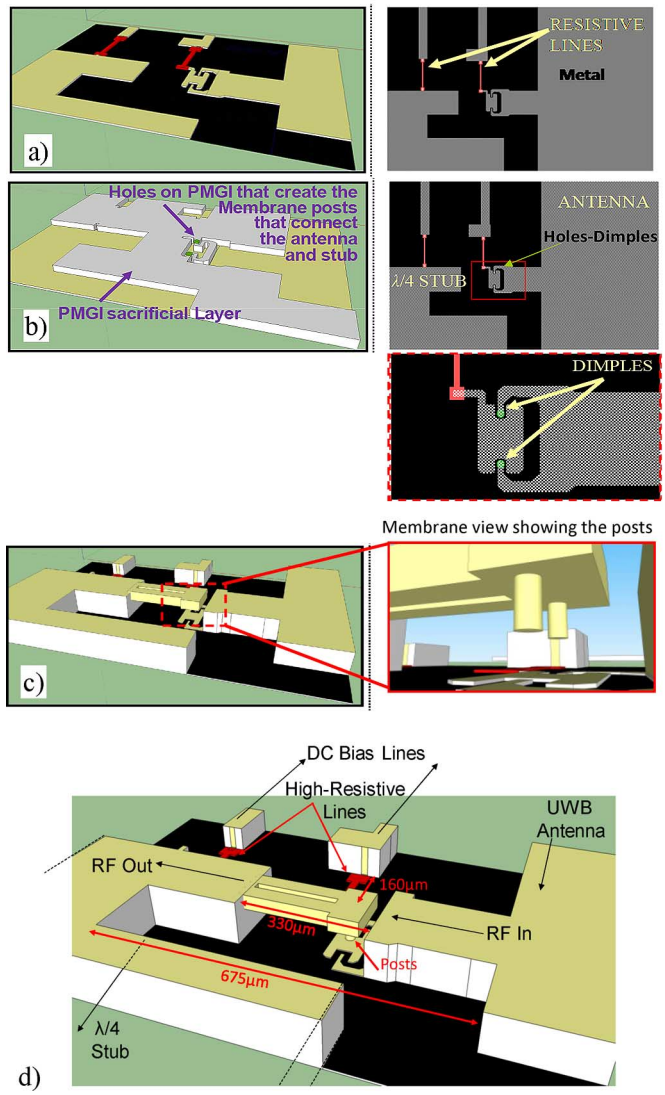

Fig. 3. (a)–(d). 3-D illustration of the major fabrication stages and masks to integrate the RF-MEMS switch with the antenna.

Finally, the integrated MEMS switch and antenna are released in a CO_2 critical point dryer (Figs. 3(c),(d)). Fig. 4 shows photos and dimensions of the fabricated device and switches. The entire fabrication process can be completed in less than 24 hours in a commercial facility.

V. Measurement Setup and Results

The series ohmic-contact cantilever MEMS act as relays that activate or deactivate the stubs when the 30-Volt actuation voltage is applied. The equivalent circuit of the MEMS 'on' is a small series inductance L_1 and resistance R_1, in parallel with a small capacitance C_1 (Fig. 5(a)). In the 'off' state, the MEMS present an additional (small) capacitance C_1' in series, which prevents the RF from entering the stub (Fig. 5(b)) [25]. The circuit model of the resonant stub is a parallel *RLC* [24] and typical values that satisfy it are: $R_2 = 250\ \Omega$, $L_2 = 0.5$ nH and $C_2 = 1.7$ pF. In Fig. 6 we see the analytical (calculated), simulated, and measured impedance of the equivalent circuit.

The antenna $|S_{11}|$ and radiation patterns were measured with MEMS 'on' and 'off', using a 10 MHz to 67 GHz Agilent

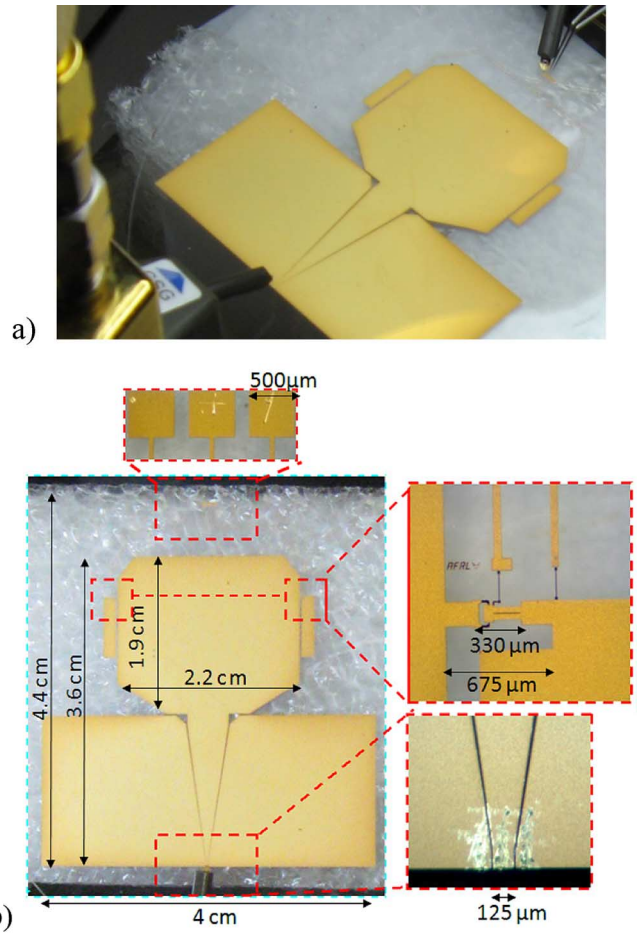

Fig. 4. (a) The fabricated antenna with MEMS during measurements showing the RF and DC probes. The circular Quartz wafer is almost transparent. The DC bias lines can be seen in very light golden color. (b) Top view showing the MEMS switch, feeding taper (some wear is due to our measurements), DC bias pads, and antenna dimensions. First appeared in [23].

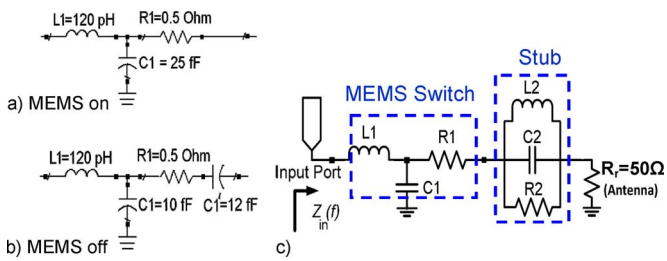

Fig. 5. Equivalent circuits: (a) RF MEMS switch 'on', (b) 'off', and (c) ideal UWB antenna, as a $R_r = 50\ \Omega$ load, with the MEMS on and stub.

E8361C PNA network analyzer. The UWB antenna was measured from 1 GHz to 12 GHz (Fig. 7), and for better resolution at the rejected bands and to reduce the noise floor, it was re-measured from 4.8 GHz to 6.2 GHz using only 10 Hz IF bandwidth. This was omitted from [23] and increases significantly the accuracy of the measurement at the rejected frequencies. With MEMS 'off', the antenna is well-matched from 2.8 GHz to 12 GHz (Fig. 7(a)). With MEMS 'on', a strong rejection with a 2.7 dB return loss is measured at the 5.52 GHz center WLAN frequency (Fig. 7(b)), illustrating approximately 50% radiating power attenuation. Also, from 5.05 to 6.05 GHz the $|S_{11}| > -10$ dB, while from 5.13 GHz to 5.84 GHz the $|S_{11}| > -6$ dB, which shows that the other WLAN frequencies

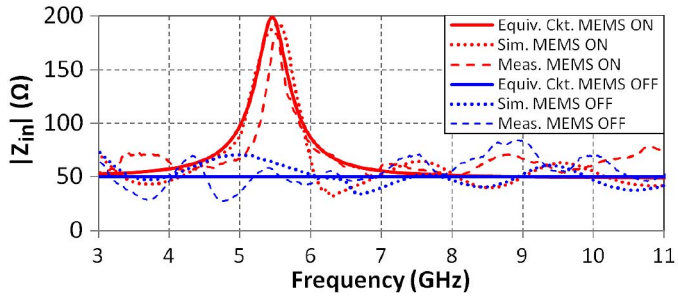

Fig. 6. Input impedance comparison between the analytical calculations, the simulations and the measurements of the reconfigurable UWB antenna with single stubs and RF-MEMS switches.

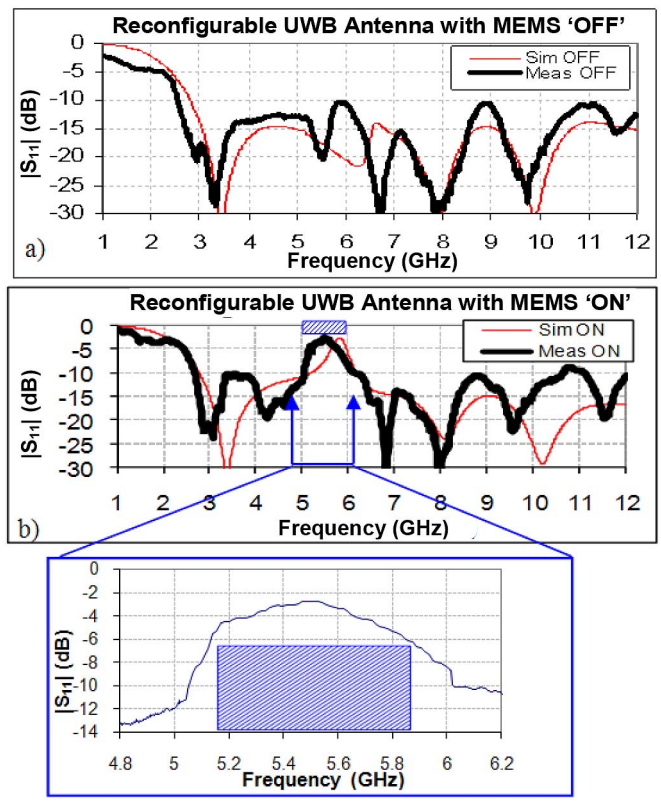

Fig. 7. (a)–(b). (a) Measured $|S_{11}|$ of the reconfigurable antenna with switches 'off', and (b) with switches 'on', showing also the 4.8 GHz to 6.2 GHz rejection region and the WLAN bands.

are also attenuated by more than 25%, and with sharp roll-off. A small shift from the simulated response, although minor for the number of materials and layers of the simulated, integrated unpackaged MEMS and bias lines, can be due to the proximity of the RF probe to the antenna or to fabrication inaccuracies.

The radiation patterns were measured during biasing using a custom made 1.5 GHz to 67 GHz reconfigurable antenna measurement platform (RecAMP), which was designed and built for this purpose, and can be controlled manually or through Labview. The platform is shown in Fig. 8 and consists of a lightweight arm counterbalanced by a mass close to the pivot to balance the gravitational forces of the assembly so that the motor can turn it wobble-free, while keeping the moment of inertia low for better start/stop response.

The measured and simulated E- and H-plane patterns are shown in Fig. 9. The 4 and 7 GHz E-plane is toroidal and the

Fig. 8. Photo of the reconfigurable antenna measurement system (RecAMP) during the pattern measurement of the reconfigurable antenna.

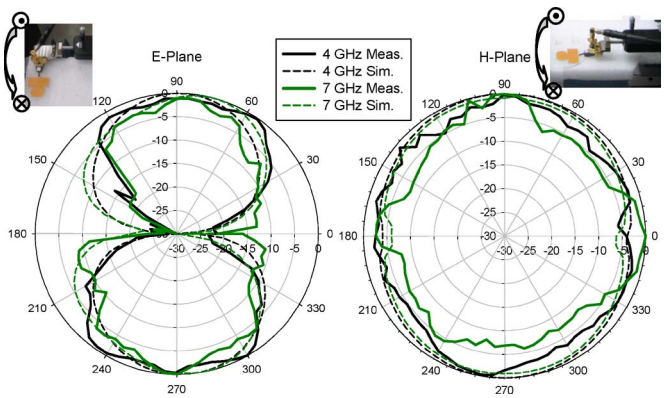

Fig. 9. E- and H-plane at 4 and 7 GHz, measurements and simulations.

H-plane omnidirectional, as expected for this type of antenna. The measured E-plane pattern attenuates from 130° to 180° and inevitably deviates from the (symmetric) simulations because of reflections at grazing angles by the right-angled RF probe adapter.

The measured and simulated E- and H-plane patterns are shown in Fig. 9. The 4 and 7 GHz E-plane is toroidal and the H-plane omnidirectional, as expected for this type of antenna. The measured E-plane pattern attenuates from 130° to 180° and inevitably deviates from the (symmetric) simulations because of reflections at grazing angles by the right-angled RF probe adapter.

The measured patterns with MEMS 'on' and 'off' at 5.5 GHz (center of the rejected band) are also similar to the simulations, as shown in Fig. 10. With MEMS 'on', the antenna radiation intensity is smaller on all directions and its broadside gain is reduced by more than 3 dB.

Gain measurements are reported in Fig. 11 at 5.0, 5.5 and 6.0 GHz, and confirm the 3.38 dB gain reduction at 5.5 GHz where $G_{off} = 2.8$ dBi while $G_{on} = -0.58$ dBi. The average gain of the antenna is in the range of 1.5 dBi to 3 dBi, which

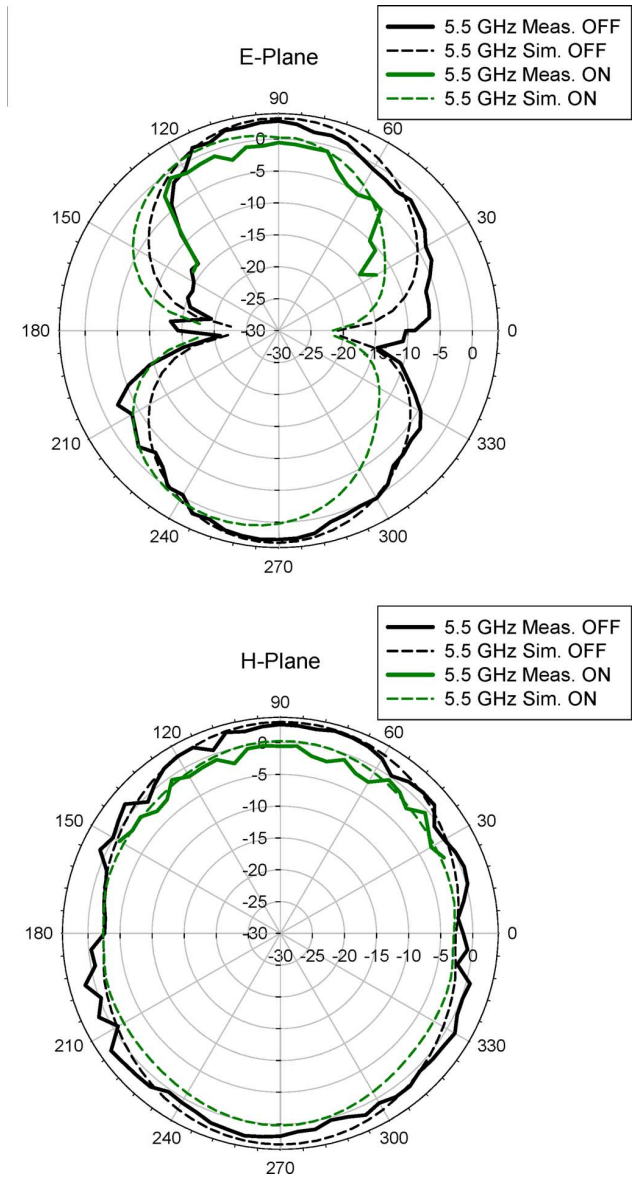

Fig. 10. E- and H-plane gain patterns at 5.5 GHz (the central rejection frequency) for RF-MEMS 'on' and 'off', measurements and simulations.

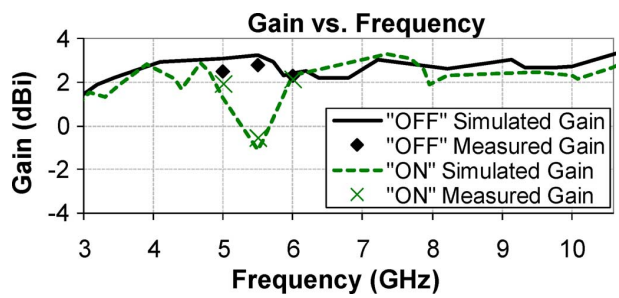

Fig. 11. Measured and simulated gain of the antenna with MEMS.

is good for an omnidirectional receiver, and frequencies outside the rejected WLAN band are not attenuated.

It is known that 'perfect matching' using a single resonance circuit can be achieved only at a single frequency [26]. Broader bandwidth often implies 'imperfect' matching. Similarly 'perfect rejection' over a wide range of frequencies cannot be achieved with a single-resonance structure like the resonant

$\lambda/4$ stub. Since the objective here is the rejection of a wide range of frequencies (i.e., the entire WLAN—similar to an ideal brick-wall filter), the level of rejection cannot be very high but can reach the levels of an optimized simulated model. As an example, in [2] a 20 dB gain reduction is achieved but at a very narrow (100 MHz) bandwidth. However, here the gain reduction is more than 3 dB and it covers a six times larger bandwidth.

The measured results are very satisfactory because the rejected bandwidth (5.15 to 5.825 GHz) and maximum level of rejection ($|S_{11}| = -2.7$ dB) are comparable or better than prior studies of band-reject antennas aiming similar functionalities with or without facing the challenges of MEMS integration and of sharp roll-off, and that rejected significantly narrower bandwidths (e.g., [2], [3], [5], [6], [10], [12], [13]). As an example, the MEMS-based UWB antenna [13] rejects approximately 400 MHz bandwidth with peak return loss 2.5 dB (while the proposed device rejects approximately 675 MHz bandwidth with comparable peak return loss 2.7 dB). It also compares well with fixed band-notched UWB antennas such as (for example) [6] where a 600 MHz bandwidth is rejected with 4.4 dB maximum return loss, [5] where 200 MHz are rejected with 5 dB peak return loss, and [12] where the curved multi-band-rejection mechanism rejects 5.05–5.8 GHz with approximately 10 dB return loss and achieves a peak of 3 dB return loss in the 1st WLAN band (5.05 to 5.6 GHz) and a peak of 4.4 dB return loss in the 2^{nd} WLAN band (5.6 to 5.8 GHz).

VI. Discussion and Conclusions

The design and successful integration of MEMS with a band-reject UWB antenna for on-demand WLAN rejection was presented. The antenna consists of linear sections and is easy to replicate and fine-tune for other applications. It is conformal, single-sided, and the MEMS are monolithically integrated on its surface.

The high-resistive lines, that were developed, were deposited at low temperature, which makes them attractive for many other temperature-sensitive substrates such as LCP (as the deposition pressure does not induce a phase change) and even paper.

This is one of the few works where a MEMS integrated antenna is completely characterized at a university facility. Measuring the antenna pattern during biasing presented interesting challenges because the RF and DC probes and the DUT cannot rotate. A measurement platform (RecAMP) was developed to enable this capability. This platform can also be used to measure other reconfigurable antennas up to 67 GHz.

The proposed antenna can be used in next generation WLAN and low-power UWB systems that will minimize interference to nearby receivers, as well as in high-performance and highly versatile cognitive radios that have low-loss. The on-demand rejection of WLAN interfering signals can lead to UWB and WLAN links with increased S/N ratio, higher capacity and throughput, and thus can improve the quality, the efficiency and the S/N ratio of UWB communication links in cognitive radio and in dense WLAN environments.

References

[1] Fed. Commun. Comm., "First report and order, revision of part 15 of the commission's rule regarding ultra wideband transmission systems," FCC 02-48 Apr. 22, 2002.

[2] K.-H. Kim, Y.-J. Cho, S.-P. Hwang, and S.-O. Park, "Band-notched UWB planar monopole antenna with two parasitic patches," *Electron. Lett.*, vol. 41, no. 14, pp. 783–785, Jul. 7, 2005.

[3] W. J. Lui, C. H. Cheng, and H. B. Zhu, "Improved frequency notched ultrawideband slot antenna using square ring resonator," *IEEE Trans. Antennas Propag.*, vol. 55, no. 9, pp. 2445–2450, 2007.

[4] T. Yang, W. A. Davis, and W. L. Stuzman, "Folded-notch dual band ultra-wideband antenna," in *Proc. IEEE APS Int. Symp.*, 2005, vol. 1B, pp. 520–523.

[5] T. Dissanayake and K. P. Esselle, "Design of slot loaded band-notched UWB antennas," in *Proc. IEEE APS Int. Symp.*, Jul. 2005, vol. 1b, pp. 545–548.

[6] K. Chung, J. Kim, and J. Choi, "Wideband microstrip-fed monopole antenna having frequency band-notch function," *IEEE Microw. Wireless Comp. Lett.*, vol. 15, no. 11, pp. 766–768, Nov. 2005.

[7] Y.-C. Lin and K.-J. Hung, "Compact ultrawideband rectangular aperture antenna and band-notched designs," *IEEE Trans. Antennas Propag.*, vol. 54, no. 11, pp. 3075–3081, Nov. 2006, pt. 1.

[8] H. G. Schantz, G. Wolenec, and E. M. Myszka, "Frequency notched UWB antennas," in *Proc. IEEE Conf. UWB Systems & Tech.*, VA, Nov. 16–19, 2003, pp. 214–218.

[9] D. E. Anagnostou, S. Nikolaou, H. Kim, B. Kim, M. Tentzeris, and J. Papapolymerou, "Dual band-notched ultra-wideband antenna for 802.11a LAN environments," in *Proc. IEEE APS Int. Symp.*, Jun. 10–15, 2007, pp. 4621–4624.

[10] K. S. Ryu and A. A. Kishk, "UWB antenna with single or dual band-notches for lower WLAN band upper WLAN band," *IEEE Trans. Antennas Propag.*, vol. 57, no. 12, pp. 3942–3950, Dec. 2009.

[11] W. T. Li, X. W. Shi, and Y. Q. Hei, "Novel planar UWB monopole antenna with triple band-notched characteristics," *IEEE Antennas Wireless Propag. Lett.*, vol. 8, pp. 1094–1098, 2009.

[12] C.-C. Lin, J. Peng, and R. W. Ziolkowski, "Single, dual and tri-band-notched ultrawideband (UWB) antennas using capacitively loaded loop (CLL) resonators," *IEEE Trans. Antennas Propag.*, pp. 102–109, Jan. 2012.

[13] S. Nikolaou, N. D. Kingsley, G. E. Ponchak, J. Papapolymerou, and M. M. Tentzeris, "UWB elliptical monopoles with a reconfigurable band notch using MEMS switches actuated without bias lines," *IEEE Trans. Antennas Propag.*, vol. 57, no. 8, pp. 2242–2251, Aug. 2009.

[14] J. Perruisseau-Carrier, P. Carrera, and P. Miskovsky, "Modeling, design and characterization of a very wideband slot antenna with reconfigurable band rejection," *IEEE Trans. Antennas Propag.*, vol. 58, no. 7, pp. 2218–2226, Jul. 2010.

[15] X. Artiga, J. Perruisseau-Carrier, P. Pardo-Carrera, I. Llamas-Garro, and Z. Brito-Brito, "Halved Vivaldi antenna with reconfigurable band rejection," *IEEE Antennas Wireless Propag. Lett.*, vol. 10, pp. 56–58, 2011.

[16] M. R. Hamid, P. Gardner, P. S. Hall, and F. Ghanem, "Review of reconfigurable Vivaldi antennas," in *Proc. IEEE APS Int. Symp.*, Jul. 11–17, 2010, pp. 1–4.

[17] J.-C. Chiao, Y. Fu, I. M. Chio, M. DeLisio, and L.-Y. Lin, "MEMS reconfigurable vee antenna," in *Proc. IEEE MTT-S Int. Microw. Symp. Dig.*, Anaheim, CA, Jun. 13–19, 1999, vol. 4, pp. 1515–1518.

[18] C. W. Jung, M.-J. Lee, G. P. Li, and F. De Flaviis, "Reconfigurable scan-beam single-arm spiral antenna integrated with RF-MEMS switches," *IEEE Trans. Antennas Propag.*, vol. 54, no. 2, pp. 455–463, Feb. 2006, pt. 1.

[19] D. E. Anagnostou, G. Zheng, M. Chryssomallis, J. Lyke, G. Ponchak, J. Papapolymerou, and C. G. Christodoulou, "Design, fabrication and measurements of an RF-MEMS-based self-similar reconfigurable antenna," *IEEE Trans. Antennas Propag.*, vol. 54, no. 2, pp. 422–432, Feb. 2006, Pt 1.

[20] B. A. Cetiner, G. R. Crusats, L. Jofre, and N. Biyikli, "RF MEMS integrated frequency reconfigurable annular slot antenna," *IEEE Trans. Antennas Propag.*, vol. 58, no. 3, pp. 626–632, Mar. 2010.

[21] E. Erdil, K. Topalli, M. Unlu, O. A. Civi, and T. Akin, "Frequency tunable microstrip patch antenna using RF MEMS technology," *IEEE Trans. Antennas Propag.*, vol. 55, no. 4, pp. 1193–1196, Apr. 2007.

[22] N. Kingsley, D. E. Anagnostou, M. Tentzeris, and J. Papapolymerou, "RF MEMS sequentially reconfigurable Sierpinski antenna on a flexible organic substrate with novel DC-biasing technique," *IEEE/ASME J. Microelectromech. Syst.*, vol. 16, no. 5, pp. 1185–1192, Oct. 2007.

[23] N. Sepúlveda, D. E. Anagnostou, M. T. Chryssomallis, and J. L. Ebel, "Integration of RF-MEMS switches with a band-reject reconfigurable ultra-wideband antenna on SiO_2 substrate," in *Proc. IEEE APS Int. Symp.*, Toronto, ON, Canada, Jul. 11–17, 2010, pp. 1–4.
[24] A. A. Gheethan and D. E. Anagnostou, "Dual band-reject UWB antenna with sharp rejection of narrow and closely-spaced bands," *IEEE Trans. Antennas Propag.*, vol. 60, no. 4, pp. 2071–2076, Apr. 2012.
[25] G. Zheng, "Low power reconfigurable microwave circuits using rf mems switches for wireless systems," Ph.D. dissertation, Georgia Inst. Technol., Atlanta, GA, USA, May 2005.
[26] S. R. Best, , J. L. Volakis, Ed., "Chapter 6: Electrically small antennas," in *Antenna Engineering Handbook*, 4th ed. New York, NY, USA: McGraw-Hill, 2007.

Dimitris E. Anagnostou (S'98–M'05–SM'10) received the B.S.E.E. degree from the Democritus University of Thrace, Greece, in 2000, and the M.S.E.E. and Ph.D. degrees from the University of New Mexico, Albuquerque, NM, USA, in 2002 and 2005, respectively.

From 2005 to 2006, he was a Postdoctoral Fellow at the Georgia Institute of Technology, Atlanta, GA, USA. In 2007 he joined the faculty of the Electrical and Computer Engineering Department, South Dakota School of Mines and Technology, where he is currently an Associate Professor. In 2011 he was an AFRL Summer Faculty Fellow with the Kirtland Air Force Base, NM, USA. He has authored or coauthored more than 80 papers published in refereed journals and symposia proceedings and he holds one U.S. patent on MEMS reconfigurable antennas. His interests include reconfigurable, autonomous, flexible, electrically-small and miniaturized antennas and arrays; phase-change materials; analytical design methods and equivalent circuits of antennas and microwave components; metamaterial applications; direct-write; security printing; "green" RF electronics on paper and organic substrates; applications of artificial dielectrics and superstrates; antennas on PV-cells; RF-MEMS; propagation in tunnels; and microwave packaging.

Dr. Anagnostou is a member of Eta Kappa Nu, ASEE, and of the Technical Chamber of Greece. He received the DARPA Young Faculty Award in 2011 and the IEEE AP-S John Kraus Antenna Award in 2010. He also received the honored faculty award by the South Dakota School of Mines and Technology in 2010, 2011, and 2012. In 2006, he was recognized as a Distinguished Scientist by the Hellenic Ministry of Defense. He serves as an Associate Editor for the IEEE TRANSACTIONS ON ANTENNAS AND PROPAGATION and the Springer *International Journal of Machine Learning and Cybernetics*, as a member of the IEEE AP-S Education Committee, and as a member of the Technical Program Committee and Session Chair for IEEE AP-S International Symposia. He has given two workshop presentations at IEEE AP-S and IEEE MTT-S International Symposia, and co-organized a convened Session in EuCAP 2014 on Reconfigurable Systems.

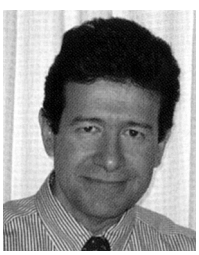

Michael T. Chryssomallis (M'88–SM'00) received the diploma and the Ph.D. degree from Democritus University of Thrace, Greece, in 1981 and 1988, respectively, both in electrical engineering.

In 1982, he joined Democritus University as a Scientific Collaborator and he is currently an Associate Professor. He worked with the Communications Group (Director, Prof. P. S. Hall) of the University of Birmingham, for the period of October 1997 to January 1998, in the areas of active antennas, and with the Wireless Group (Director Prof. C. G. Christodoulou) of the University of New Mexico, for the periods of April to June 2000, and April to July 2002, in the areas of microstrip antennas and arrays, and smart antennas. His current research interests are in the areas of small antennas, RF-MEMS, smart antennas, algorithms of beamforming and angle-of-arrival estimation, and propagation-channel characterization. He is the author or co-author of 60 journal papers and conference proceedings, which have more than 350 citations. He has participated in 16 research projects, is the author or coauthor of three book chapters in English and translated an English book into Greek.

Dr. Chryssomallis serves as a reviewer for several publications of the IEEE and IEE.

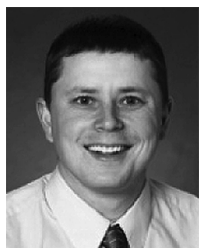

Benjamin D. Braaten (S'02–M'09) received the Ph.D. degree in electrical engineering from North Dakota State University, Fargo, ND, USA, in 2009.

During the fall semester 2009, he held a postdoctoral research position at the South Dakota School of Mines and Technology, Rapid City, SD, USA. Currently, he is an Assistant Professor in the Electrical and Computer Engineering Department at North Dakota State University. His research interests include printed antennas, conformal self-adapting antennas, microwave devices, topics in EMC, and methods in computational electromagnetics.

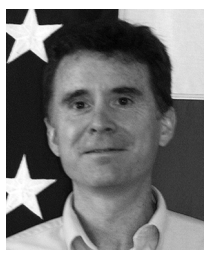

John L. Ebel (M'13) received the B.S. and M.Eng. degrees in electrical engineering from Cornell University, Ithaca, NY, USA, in 1984 and 1985, respectively, and the Ph.D. degree in electrical and computer engineering from Carnegie Mellon University, Pittsburgh, PA, US, in 1998.

He is a Research Engineer in the Sensors Directorate of the Air Force Research Laboratory (AFRL) at Wright Patterson Air Force Base, OH, USA. At AFRL since 1985, he is currently the Technical Advisor for the Electron Devices Branch within the Sensors Directorate. Earlier research interests included development of MEMS devices for microwave applications, scanning probe microscopy, pseudomorphic high-electronmobility transistors, physical device modeling, and the VHSIC hardware description language (VHDL) development.

Nelson Sepúlveda (S'05–M'06–SM'11) received the B.S. degree in electrical and computer engineering from the University of Puerto Rico, Mayaguez, Puerto Rico, in 2001 and the M.S. and Ph.D. degrees in electrical and computer engineering from Michigan State University, East Lansing, MI, USA, in 2002 and 2005, respectively.

During the last year of Graduate School, he attended Sandia National Laboratories as part of a fellowship from the Microsystems and Engineering Sciences Applications program. In January 2006, he joined the Electrical and Computer Engineering faculty at the University of Puerto Rico, Mayaguez, Puerto Rico. He has been a Visiting Faculty Researcher at the Air Force Research Laboratories in 2006, 2007, and 2013, the National Nanotechnology Infrastructure Network in 2008, and the Cornell Center for Materials Research in 2009, the last two being NSF-funded centers at Cornell University, Ithaca, NY, USA. In 2011, Nelson joined the Department of Electrical and Computer Engineering at Michigan State University (MSU), where he is currently an Assistant Professor. His current research interests include smart materials and the integration of such in micro-electro-mechanical systems (MEMS), with particular emphasis on vanadium dioxide (VO2) thin films, and the use of the structural phase transition for the development of smart microactuators.

Dr. Sepúlveda received the NSF CAREER Award in 2010.